THE JOURNAL OF PHYSICAL CHEMISTRY LETTERS
A JOURNAL OF THE AMERICAN CHEMICAL SOCIETY

pubs.acs.org/JPCL

Letter

Mesoscopic Pitting Oscillation-Induced Periodic Anodic Layer Electrodissolution of Au(111)

Changwei Pan,[§] Mingshuang Niu,[§] Ruijun Cui, Lianqun Li, Xinyu You, Xiao Sun, Chen Ji, Irving R. Epstein, and Qingyu Gao*

Cite This: *J. Phys. Chem. Lett.* 2021, 12, 12062–12066

Read Online

ACCESS | Metrics & More | Article Recommendations | Supporting Information

ABSTRACT: The electrodissolution of Au(111) in anaerobic cupric/ammonia/thiosulfate solutions, typical of a non-equilibrium dissipative system, was investigated via in situ electrochemical atomic force microscopy. At a specific initial concentration ratio of aqueous ammonia to cupric ions, the pit number and average pit area increase autocatalytically, while the pit depth increases monotonically during dissolution. A further increase in this initial concentration ratio leads to oscillatory dynamics in the pit number and average pit area while the pit depth fluctuates between one and two atoms. Mechanistic analysis indicates that alternation between formation and dissolution of a sulfur film results in periodic pitting, which produces gold dissolution layer by layer. This work presents a new dissolution mode, i.e., periodic layer dissolution generated by oscillatory pitting processes in addition to a pitting mode with a continually increasing depth, and the use of high initial concentration ratios of ammonia to cupric ion to accelerate the elimination of passivating sulfur film for Au dissolution.

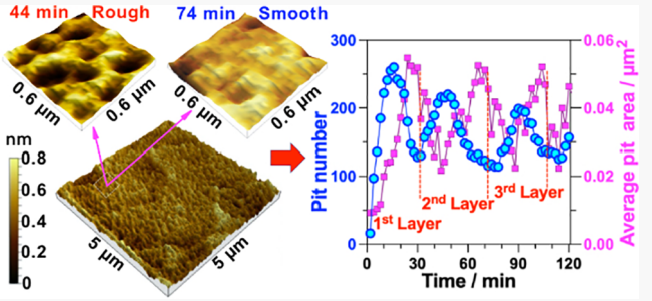

Metal dissolution, often involved in corrosion[1] and leaching,[2] can display two basic modes, i.e., pitting[3−7] and layer dissolution[8,9] including wave dissolution (i.e., step flow).[10,11] The pitting process in steel has been described as random, sporadic, and stochastic.[3] Hudson et al.[4] observed autocatalytic formation of steel pits: the sudden onset of corrosion is accompanied by the formation and growth of regions with multiple metastable pits. This process has been reproduced well by a stochastic model in which the probability of pit formation depends on the local film damage, the concentration of aggressive species pit releases, and the ohmic drop around active pits.[4,12] If a protective layer is repeatedly formed and dissolved, metallic dissolution may exhibit not only autocatalytic pitting resulting from a mechanism similar to that of stainless steel[4] but also oscillatory dynamics and pit-mediated periodical layer dissolution. Au(111) electrodissolution in cupric/ammonia/thiosulfate solutions occurs through anodic reaction 1 with concomitant reaction 2.[13]

$$Au + 2S_2O_3^{2-} = Au(S_2O_3)_2^{3-} + e^- \quad (1)$$

$$2S_2O_3^{2-} = S_4O_6^{2-} + 2e^- \quad (2)$$

However, the dissolution of gold in thiosulfate solutions is relatively complicated due to a passive sulfur layer,[14,15] which is formed via reactions 3 and 4 and prevents the electrochemical reaction of surface gold atoms with thiosulfate. More specifically, the tetrathionate produced in reaction 2 reacts with thiosulfate to generate higher polythionates, such as pentathionate, and hexathionate, as shown in reaction 3.[16] These compounds are highly unstable at pH >9 and decompose to elemental sulfur, as shown in reactions 4 and 5.[17,18] The elemental sulfur deposited on the Au(111) surface acts as a passivating film and prevents the contact of Au^0 atoms with thiosulfate, thus suppressing the dissolution of Au(111).

$$S_4O_6^{2-} + mS_2O_3^{2-} = S_{4+m}O_6^{2-} + mSO_3^{2-} \quad (3)$$

$$S_{4+m}O_6^{2-} = S_{3+m}O_6^{2-} + S \quad (4)$$

$$2S_{4+m}O_6^{2-} + 6OH^- = 5S_2O_3^{2-} + 2(m-1)S + 3H_2O \quad (5)$$

Reaction 1 is inhibited by the sulfur film. The addition of ammonia and cupric ions, which form cupric tetraamine, may dissolve the passive film composed of sulfur species on the surface,[15] producing Cu(I) species according to reaction 6, which has a strongly favorable Gibbs free energy of −501.94 kJ mol^{-1}.

Received: October 7, 2021
Accepted: December 13, 2021
Published: December 15, 2021

$$4[Cu(NH_3)_4]^{2+} + 2S + 11S_2O_3^{2-} + 6OH^- = 4[Cu(S_2O_3)_3]^{5-} + 16NH_3 + 3H_2O \quad (6)$$

The Cu(I) species that form during elemental sulfur dissolution can be reoxidized to Cu(II) on the electrode surface through reaction 7 where n can be 2 or 3. The redox potentials for the reaction are calculated to be 0.14 V (n = 2) and 0.224 V (n = 3) [standard hydrogen electrode (SHE)].[13]

$$Cu(S_2O_3)_n^{5-} + 4NH_3 \rightarrow Cu(NH_3)_4^{2+} + nS_2O_3^{2-} + e^- \quad (7)$$

The repeated formation of a cupric tetraamine complex could be repeatedly used to eliminate passivated sulfur species on the Au(111) surface during the pitting process. This work explores possible complex behaviors during the pitting process of Au(111) bead electrodes in cupric/ammonia/thiosulfate solutions using *in situ* electrochemical atomic force microscopy (EC-AFM). Nonlinear pitting phenomena, such as autocatalytic growth and oscillations in both pit number and average pit area, are observed on Au(111) bead electrodes in thiosulfate solutions by adjusting the applied potential and the concentrations of the cupric cation and ammonia.

When the concentration of $CuSO_4$ is 3.0 mM at 86.0 mM ammonia and 0.235 V, the dissociated free Cu^{2+} ions oxidize thiosulfate to tetrathionate and then strengthen the local stability of passive sulfur films via reactions 3−5, producing an autocatalytic formation of pits to an approximate saturated plateau in the pit number and average pit area, as shown in Figure 1 and Movie S1. Figure 1a shows a three-dimensional (3D) AFM image of the Au(111) plane at 60 min with a constant pit number. Figure 1b shows the autocatalytic increase in the pit number (blue) with time. An induction process is observed in the initial stage of dissolution; a rapid growth process occurs after 22 min, and then a stable value is reached after ~40 min. From the time curve of the average pit area (purple) shown in Figure 1b and Movie S1, the pitting area increases rapidly before 40 min and then remains stable after 40 min, which is seemingly analogous to the time evolution of the pit number in Figure 1b. However, the curve of the average pit area in Figure 1b shows significant hysteresis and even a drop between 28 and 40 min, which results from an autocatalytic increase in smaller pits. For the steady etching state after 40 min, approximately half of the probed area remains undissolved and exists as peaks of hills. Figure 1c shows the continual increase in the average pit depth over time. However, there is a time plateau appearing between 65 and 90 min, which is possibly due to dissolution of a new sulfur film forming at the bottom of the inner pits. This is different from the autocatalytic increase to steady state of the pit number and the average pit area.

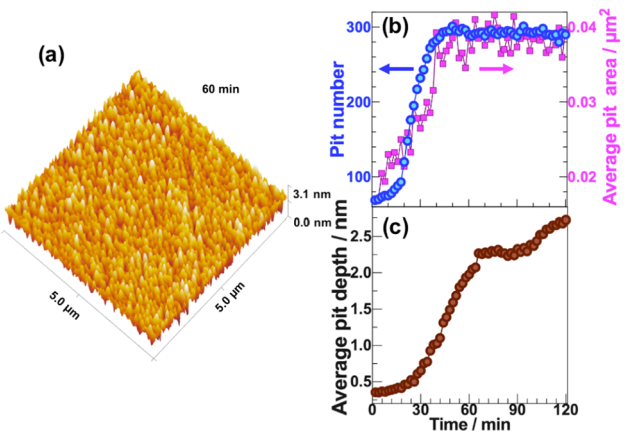

Figure 1. Autocatalytic formation of pits during anaerobic electrodissolution of Au(111) bead electrodes. (a) 3D AFM image of the Au(111) plane in a solution of 50.0 mM thiosulfate, 86.0 mM ammonia, and 3.0 mM cupric cations at an applied potential of 0.235 V and 60 min. (b) Pit number (blue) and average pit area (purple) vs time. (c) Average pit depth vs time. The image size is 5 μm × 5 μm.

When we decreased the concentration of $CuSO_4$ from 3.0 to 1.0 mM at an applied potential of 0.235 V, we observed a transition from autocatalytic growth to oscillations of pitting, as shown in Figure S1. Decreasing the potential causes the obvious oscillations in both pit number and average pit area (Figure S2). Therefore, we decreased the applied potential to the open circuit potential (OCP, 0.20 V vs SHE) to investigate pitting dissolution, as shown in Figure 2 and Movie S2. Pitting oscillation-induced layer dissolution can be inferred in this system from four points as follows. First, a 3D movie (Movie S2) shows the dissolution process in which each point of the layer was dissolving and their relative heights were changing dynamically. Second, the pit number and the average pit area display antiphase (i.e., 180° out of phase) oscillations as shown in panels a and b of Figure 2, indicating that the average pit area

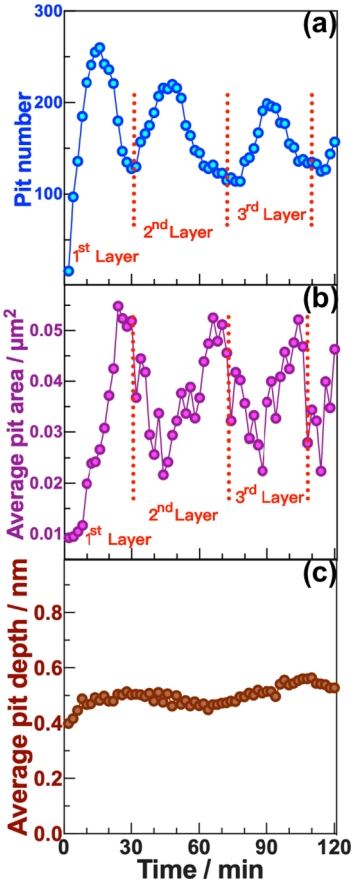

Figure 2. Time evolution of pit number, average pit depth, and pit area during the anaerobic electrodissolution of Au(111) bead electrodes. Plots of (a) the oscillating pit number, (b) the average pit area, and (c) the average pit depth vs time under potentiostatic conditions at OCP (0.20 V vs SHE). $[S_2O_3^{2-}]_0$ = 50.0 mM. $[Cu^{2+}]_0$ = 1.0 mM. $[ammonia]_0$ = 86.0 mM. The image size is 5 μm × 5 μm.

https://doi.org/10.1021/acs.jpclett.1c03300
J. Phys. Chem. Lett. 2021, 12, 12062−12066

and the pit number reach the maximum and minimum, respectively, when previous layer dissolution just ends. Third, the average pit depths approach two atomic layers (~0.28 nm per Au) during oscillatory dissolution as shown in Figure 2c, indicating the individual pit depth fluctuates between one and two Au atoms. If layer dissolution does not occur, the average pit depth would increase monotonously after every oscillatory period of pit dissolution. Finally, the dissolution of a layer can be determined by identifying the terraces of Au(111) that show low average surface roughness values (Figure S3) with a relatively flattened surface (Figure S4) after one oscillatory period. Here, pits of the next layer were born during one pitting oscillation of previous layer dissolution, so minimal pit numbers during oscillations are not zero as shown in Figure 2a. To clearly observe evolution of one-layer dissolution, the applied potential was decreased to 0.195 V versus SHE as shown in Movie S3, which displays the appearance, growth, and merging of pits. The times at which layer dissolution is completed are marked by red dotted lines in Figure 2a, where the average pit area decreases suddenly from its maximum value (Figure 2b), and after those lines autocatalytic growth in the pit number (i.e., a large number of new smaller pits are formed) results in a decrease in the average pit area to a minimum corresponding to the next maximum of the pit number. When the applied potential was increased to 0.21 V versus SHE as shown in Movie S4 and Figure S5, more obvious oscillations of the average surface roughness were observed in 50 mM thiosulfate solutions containing 86 mM ammonia and 2.0 mM cupric ions.

We analyzed the local evolution of the pits in one period of oscillation by investigating the morphological evolution for the increase and decrease in the pit number, with pitting time, as shown in Figure 3 and Movie S5. The pit number in the region of

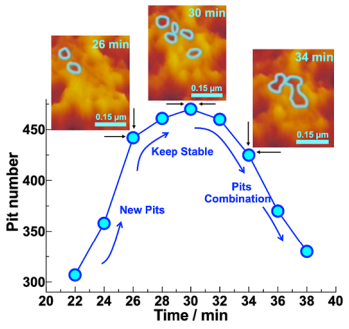

Figure 3. Local evolution of the pits during one period of pit number oscillations on the Au(111) bead electrode. $[S_2O_3^{2-}]_0$ = 50.0 mM. $[Cu^{2+}]_0$ = 1.0 mM. [ammonia]$_0$ = 200.0 mM. The applied potential is fixed at 0.26 V.

observation oscillates with the pitting time. In the stage from 22 to 28 min in which the pit number increases, new pits randomly emerge around the already existing pits. In the stage from 28 to 32 min, the pit number remains around its maximum. Finally, in the stage from 32 to 38 min, the pit number decreases, mainly due to the merging of two or more adjacent pits.

The coupling of the electrochemical dissolution of gold with formation and elimination of a sulfur film gives rise to nonlinear phenomena, such as autocatalytic pitting at higher $CuSO_4$ concentrations under higher applied potentials and pitting oscillation-induced layer dissolution at lower applied potentials and low $CuSO_4$ concentrations. The following qualitative mechanistic analysis summarizes our understanding of the non-equilibrium behaviors observed on a mesoscopic level. In stainless steel corrosion, only autocatalytic pitting during was observed, probably because the passive film cannot be dissolved repeatedly under the experimental condition.[4] The gold in a cyanide or chloride solution displays homogeneous or wave-type (i.e., step flow) layer dissolution due to the lack of a passive film barrier. Strongly adsorbed chloride,[8−10,19] cyanide,[20] or thiourea[11] can significantly enhance surface dissolution. These species cannot be oxidized at the potential of gold dissolution; i.e., the oxidation potentials of chloride, cyanide, and thiourea are higher than that of gold dissolution. Therefore, no passivation layer preventing the dissolution of gold can be observed in these cases. However, thiosulfate is electro-oxidized to tetrathionate [$E^\circ(S_4O_6^{2-}/S_2O_3^{2-})$ = 0.08 V vs SHE] before gold dissolution [$E^\circ(Au(S_2O_3)_2^{3-}/Au^0)$ = 0.153 V vs SHE][21] results in the production and deposition of elemental sulfur, inhibiting the dissolution of gold. Therefore, no electrochemical dissolution of the Au(111) electrode is observed in a simple solution containing only thiosulfate, due to the passivating sulfur film on the Au(111) electrode surface. The cupric tetraammonia complex can repeatedly dissolve elemental sulfur of the passivating film above 0.195 V vs SHE, and the exposed gold atoms react with thiosulfate to form an aurous thiosulfate complex that is released into the bulk solution. With the alternating formation and dissolution of the sulfur film, pitting oscillations and oscillation-induced layer dissolution can occur. However, if the concentration of the dissociable cupric ion from the cupric tetraammonia complex, which can enhance the passivation such as thiosulfate oxidation by cupric ion to form sulfur film (reactions 3−5), is high, dissolution of the sulfur film will be suppressed, resulting in an S-shaped autocatalytic increase to a saturated plateau rather than oscillations in the pit number and average pit area.

In summary, a new mode of Au dissolution, namely pitting oscillation-mediated periodic layer dissolution, was observed during the electrochemical pitting process on the Au(111) facet in cupric/ammonia/thiosulfate solutions in addition to a pitting mode with a continually increasing depth. A high [ammonia]$_0$/$[Cu^{2+}]_0$ ratio accelerates elimination of the passivating sulfur film. Therefore, it increases the dissolution rate of gold and should be beneficial for the extraction of gold[22−25] from ores or "urban mines" of electronic waste. For basic research, as an effective image and video technique, *in situ* electrochemical scanning probe microscopy (EC-SPM including AFM and STM) could be used to investigate complex nonlinear phenomena occurring at the mesoscopic or atomic level and to track the structural evolution of electrode surfaces for mechanistic and theoretical analysis.

■ ASSOCIATED CONTENT

Supporting Information

The Supporting Information is available free of charge at https://pubs.acs.org/doi/10.1021/acs.jpclett.1c03300.

Experimental procedures and additional experimental data (PDF)

Evolution of the Au(111) facet and autocatalytic formation of pits in an ammoniacal thiosulfate solution containing 3.0 mM Cu^{2+} ions at 0.235 V ($[S_2O_3^{2-}]_0$ = 50.0 mM, and [ammonia]$_0$ = 86.0 mM) (Movie S1) (MOV)

Evolution of Au(111) facet and pitting oscillations in a cupric/ammoniacal thiosulfate solution containing 1.0

https://doi.org/10.1021/acs.jpclett.1c03300
J. Phys. Chem. Lett. 2021, 12, 12062−12066

mM Cu^{2+} ions at OCP (0.20 V vs SHE) ($[S_2O_3^{2-}]_0$ = 50.0 mM, and $[ammonia]_0$ = 86.0 mM) (Movie S2) (MOV)

Evolution of Au(111) facet in a cupric/ammoniacal thiosulfate solution containing 1.0 mM Cu^{2+} ions at 0.195 V vs SHE ($[S_2O_3^{2-}]_0$ = 50.0 mM, and $[ammonia]_0$ = 86.0 mM) (Movie S3) (MOV)

Oscillatory dissolution of the Au(111) facet in a cupric/ammoniacal thiosulfate solution containing 2.0 mM Cu^{2+} ions at 0.21 V ($[S_2O_3^{2-}]_0$ = 50.0 mM, and $[ammonia]_0$ = 86.0 mM) (Movie S4) (MOV)

Evolution of the local pits and the pit number on an Au(111) facet in a cupric/thiosulfate solution containing 200.0 mM ammonia at 0.26 V ($[S_2O_3^{2-}]_0$ = 50.0 mM, and $[Cu^{2+}]_0$ = 1.0 mM) (Movie S5) (MOV)

AUTHOR INFORMATION

Corresponding Author

Qingyu Gao − *Department of Chemical Engineering, China University of Mining and Technology, Xuzhou 221116, P. R. China;* orcid.org/0000-0002-5520-0240; Email: gaoqy@cumt.edu.cn

Authors

Changwei Pan − *Department of Chemical Engineering, China University of Mining and Technology, Xuzhou 221116, P. R. China*

Mingshuang Niu − *Department of Chemical Engineering, China University of Mining and Technology, Xuzhou 221116, P. R. China*

Ruijun Cui − *Department of Chemical Engineering, China University of Mining and Technology, Xuzhou 221116, P. R. China*

Lianqun Li − *Department of Chemical Engineering, China University of Mining and Technology, Xuzhou 221116, P. R. China*

Xinyu You − *Department of Chemical Engineering, China University of Mining and Technology, Xuzhou 221116, P. R. China*

Xiao Sun − *Department of Chemical Engineering, China University of Mining and Technology, Xuzhou 221116, P. R. China*

Chen Ji − *Department of Chemical Engineering, China University of Mining and Technology, Xuzhou 221116, P. R. China*

Irving R. Epstein − *Department of Chemistry and Volen Center for Complex Systems, Brandeis University, Waltham, Massachusetts 02454-9110, United States;* orcid.org/0000-0003-3180-4055

Complete contact information is available at: https://pubs.acs.org/10.1021/acs.jpclett.1c03300

Author Contributions

[§]C.P. and M.N. contributed equally to this work.

Notes

The authors declare no competing financial interest.

ACKNOWLEDGMENTS

This work was supported by the National Natural Science Foundation of China (Grants 21773304 and 22120102001), the U.S. National Science Foundation (Grant CHE-1856484), and the Fundamental Research Funds for the Central Universities (Grant 2019XKQYMS77).

REFERENCES

(1) Renner, F. U.; Stierle, A.; Dosch, H.; Kolb, D. M.; Lee, T. L.; Zegenhagen, J. Initial Corrosion Observed on the Atomic Scale. *Nature* **2006**, *439*, 707−710.

(2) Owens, B. Mining: Extreme Prospects. *Nature* **2013**, *495*, S4−S6.

(3) Ryan, M. P.; Williams, D. E.; Chater, R. J.; Hutton, B. M.; McPhail, D. S. Why Stainless Steel Corrodes. *Nature* **2002**, *415*, 770−774.

(4) Punckt, C.; Bolscher, M.; Rotermund, H. H.; Mikhailov, A. S.; Organ, L.; Budiansky, N.; Scully, J. R.; Hudson, J. L. Sudden Onset of Pitting Corrosion on Stainless Steel as a Critical Phenomenon. *Science* **2004**, *305*, 1133−1136.

(5) Hersbach, T. J. P.; Yanson, A. I.; Koper, M. T. M. Anisotropic Etching of Platinum Electrodes at the onset of Cathodic Corrosion. *Nat. Commun.* **2016**, *7*, 12653.

(6) Lasaga, S. C.; Luttge, A. Variation of Crystal Dissolution Rate Based on a Dissolution Stepwave Model. *Science* **2001**, *291*, 2400−2404.

(7) Merola, C.; Cheng, H.-W.; Schwenzfeier, K.; Kristiansen, K.; Chen, Y.-J.; Dobbs, H. A.; Israelachvili, J. N.; Valtiner, M. In situ Nano- to Microscopic Imaging and Growth Mechanism of Electrochemical Dissolution (e.g., Corrosion) of a Confined Metal Surface. *Proc. Natl. Acad. Sci. U. S. A.* **2017**, *114*, 9541−9546.

(8) Golks, F.; Krug, K.; Grunder, Y.; Zegenhagen, J.; Stettner, J.; Magnussen, O. M. High-Speed in situ Surface X-ray Diffraction Studies of the Electrochemical Dissolution of Au(001). *J. Am. Chem. Soc.* **2011**, *133*, 3772−3775.

(9) Suggs, D. W.; Bard, A. J. Scanning Tunneling Microscopic Study with Atomic Resolution of the Dissolution of Cu(111) in Aqueous Chloride Solutions. *J. Am. Chem. Soc.* **1994**, *116*, 10725−10733.

(10) Wen, R.; Lahiri, A.; Azhagurajan, M.; Kobayashi, S.-I.; Itaya, J. A new In Situ Optical Microscope with Single Atomic Layer Resolution for Observation of Electrochemical Dissolution of Au(111). *J. Am. Chem. Soc.* **2010**, *132*, 13657−13659.

(11) Li, L.; Pan, C.; Shan, J.; She, W.; You, X.; Ji, C.; Gao, Q. Pit-Induced Electrochemical Layer Dissolution and Wave Propagation on an Au(111) Surface in an Acidic Thiourea Solution. *J. Phys. Chem. C* **2020**, *124*, 19112−19118.

(12) Mikhailov, A. S.; Scully, J. R.; Hudson, J. L. Nonequilibrium Collective Phenomena in the Onset of Pitting Corrosion. *Surf. Sci.* **2009**, *603*, 1912−1921.

(13) Aylmore, M. G.; Muir, D. M. Thiosulfate Leaching of Gold- A Review. *Miner. Eng.* **2001**, *14*, 135−174.

(14) Smith, S. R.; Leitch, J. J.; Zhou, C.; Mirza, J.; Li, S. B.; Tian, X.-D.; Huang, Y.; Tian, Z.; Baron, J. Y.; Choi, Y.; Lipkowski, J. Quantitative SHINERS Analysis of Temporal Changes in the Passive Layer at a Gold Electrode Surface in a Thiosulfate Solution. *Anal. Chem.* **2015**, *87*, 3791−3799.

(15) Smith, S. R.; Zhou, C.; Baron, J. Y.; Choi, Y.; Lipkowski, J. Elucidating the Interfacial Interactions of Copper and Ammonia with the Sulfur Passive Layer during Thiosulfate Mediated Gold Leaching. *Electrochim. Acta* **2016**, *210*, 925−934.

(16) Skarzynski, B.; Szczepkowski, T. W. Oxidation of Thiosulphate by Thiobacillus Thioparus. *Nature* **1959**, *183*, 1413−1414.

(17) Pan, C.; Wang, W.; Horvath, A. K.; Xie, J.; Lu, Y.; Wang, Z.; Ji, C.; Gao, Q. Kinetics and Mechanism of Alkaline Decomposition of the Pentathionate Ion by Simultaneous Tracking of Different Sulfur Species by High-Performance Liquid Chromatography. *Inorg. Chem.* **2011**, *50*, 9670−9677.

(18) Pan, C.; Liu, Y.; Horváth, A. K.; Wang, Z.; Hu, Y.; Ji, C.; Zhao, Y.; Gao, Q. Kinetics and Mechanism of the Alkaline Decomposition of Hexathionate Ion. *J. Phys. Chem. A* **2013**, *117*, 2924−2931.

(19) Trevor, D. J.; Chidsey, C. E. D.; Loiacono, D. N. In situ Scanning-Tunneling-Microscope Observation of Roughening, Annealing, and Dissolution of Gold(111) in an Electrochemical Cell. *Phys. Rev. Lett.* **1989**, *62*, 929−932.

(20) Cimatu, K.; Baldelli, S. Chemical Imaging of Corrosion: Sum Frequency Generation Imaging Microscopy of Cyanide on Gold at the Solid-Liquid Interface. *J. Am. Chem. Soc.* **2008**, *130*, 8030−8037.

(21) Bard, A. J.; Parsons, R.; Jordan, J. *Standard Potentials in Aqueous Solution*; Marcel Dekker, Inc.: New York, 1985.
(22) Raisanen, M.; Heliovaara, E.; Al-Qaisi, F.; Muuronen, M.; Eronen, A.; Liljeqvist, H.; Nieger, M.; Kemell, M.; Moslova, K.; Hamalainen, J.; Lagerblom, K.; Repo, T. Pyridinethiol-Assited Dissolution of Elemental Gold in Organic Solutions. *Angew. Chem., Int. Ed.* **2018**, *57*, 17104−17109.
(23) Cao, W.; Dai, F.; Hu, R.; Tang, B. Economic Sulfur Coversion to Functional Polythioamides through Catalyst-Free Multicomponent Polymerizations of Sulfur, Acids, and Amines. *J. Am. Chem. Soc.* **2020**, *142*, 978−986.
(24) Liu, Z.; Samanta, A.; Lei, J.; Sun, J.; Wang, Y.; Stoddart, J. F. Cation-Dependent Gold Recovery with α-Cyclodextrin Facilitated by Second-Sphere Coordination. *J. Am. Chem. Soc.* **2016**, *138*, 11643−11653.
(25) Sun, D.; Gasilova, N.; Yang, S.; Oveisi, E.; Queen, W. L. Rapid, Selective Extraction of Trace Amounts of Gold from Complex Water Mixtures with a Metal-Organic Framework (MOF)/Polymer Composite. *J. Am. Chem. Soc.* **2018**, *140*, 16697−16703.

https://doi.org/10.1021/acs.jpclett.1c03300
J. Phys. Chem. Lett. 2021, 12, 12062−12066